Polymer Bulletin (2021) 78:4849–4862
https://doi.org/10.1007/s00289-020-03345-7

ORIGINAL PAPER

Visible light-induced cationic photopolymerization by diphenyliodonium hexafluorophosphate and benzothiadiazole dyes

Ran Liu[1] · Yuanyuan Xu[1] · Lei Wang[1] · Fan Zhang[1] · Ping Chen[1] · Yaolong Li[2] · Yu Chen[1]

Received: 25 February 2020 / Revised: 17 June 2020 / Accepted: 14 August 2020 /
Published online: 19 August 2020

Abstract

New benzothiadiazole-based long-wavelength organic dyes (**Y-1** and **Y-2**) were prepared for effectively sensitizing diphenyliodonium hexafluorophosphate (IOPF) to initiate the fast curing of bisphenol-A epoxy resin (E51) under visible light, avoiding traditional UV light sources that have high energy and high radiation. **Y-1** and **Y-2** have absorption spectra extended to more than 550 nm. By using **Y-1** and **Y-2** as photosensitizers for IOPF, E51 reach high epoxy conversions of 95% under light wavelength of 470-nm irradiation. IOPF and benzothiadiazole dyes present at the same time show good visible-light initiating activity. The high curing conversions are attributed to the photoelectron transfer reaction between diphenyliodonium hexafluorophosphate and benzothiadiazole dyes, based on our photochemical and electrochemical experiments. In addition, the terminated groups or of **Y-1** (–F) and **Y-2** ($–OCH_3$) have a great influence on the photopolymerization rate of the curing systems and thermal properties of E51 after cured. In addition, E51 was even polymerized about 70% in the presence of 510-nm light filter.

Keywords Visible-light curing · Benzothiadiazole · Diphenyliodonium hexafluorophosphate · Long-wavelength organic dyes · Bisphenol-A epoxy resin

Electronic supplementary material The online version of this article (https://doi.org/10.1007/s00289-020-03345-7) contains supplementary material, which is available to authorized users.

✉ Yu Chen
cy26tj@163.com

[1] Department of Applied Chemistry, School of Chemistry and Chemical Engineering, Tianjin University of Technology, Tianjin 300384, People's Republic of China

[2] Tianjin Dage Technology Co., Ltd., Tianjin 301700, People's Republic of China

Introduction

Nowadays, light curing technologies have been widely used on coating industry, food packing and material forming and processing, e.g., 3D printing [1–5]. The light curing induced by visible light and even infrared light is more harmless to the human body than that induced by ultraviolet (UV) lights [6]. A variety of photoinitiators, dyes and other photosensitizers as well as modified monomers or prepolymers have been successfully developed to match different light wavelengths [7–9].

Diphenyliodonium hexafluorophosphate (IOPF) is a conventional cationic UV photoinitiator [10, 11]. A broader spectrum can be matched by adding dye sensitizers to improve the visible-light initiation activity of IOPF, and thus, the epoxides can be initiated to crosslink under visible light [12–14]. Epoxy resin is a common epoxides in the curing system [15–17]. Many industrial applications use epoxy resin as one of the engineering polymer materials, such as coating and adhesive substances, semiconductor manufacturing [18, 19]. The bisphenol-A type of epoxy resin (E51) is inexpensive aromatic epoxy resin. It was often used as thermal curing materials and has slow photopolymerization rate [20, 21]. Researches have been focused on promoting E51 to fast cationic photopolymerization instead of thermal curing in the past few years, due to its good properties after polymerized [22–26].

Wang et al. [22] studied the photoinitiated and thermally initiated cationic polymerizations of diglycidyl ether of bisphenol A epoxy oligomer. Abadie et al. [23] concluded suitable addition of the sulfonium salt lowered the activation energy for the bisphenol-A epoxy system. Vabrik et al. [24] successfully synthesized diglycidyl ether of bisphenol-A epoxy resin-acrylated polyurethane semi-interpenetrating polymer networks upon irradiation with ultraviolet light. Chen et al. [25] developed a two-component photoinitiator system for promoting cationic polymerization of bisphenol-A-based epoxy under visible light. Wang et al. [26] synthesized dyes to sensitize iodonium bis(4-methylphenyl)hexafluorophosphate for cationic polymerization of E51 under the laser diode at 455 nm. These results indicate that using this safe and low-cost bisphenol-A epoxy resin and its derivatives is practical in the field of light curing technology.

Dyes with different structures and absorption ranges have been reported as long-wavelength sensitizers in the visible-curing systems initiated by diphenyliodonium hexafluorophosphate [9, 27]. However, benzothiadiazole-based organic dyes are few involved. Among the dyes, benzothiadiazole is a good electron-attracting group that forms a push–pull structure with an electron-donating group. A long-conjugated molecule forms from the structure, which broadens the long-wavelength absorption spectrum. In the field of dye-sensitized solar cells, it is reported that benzothiadiazole-based dyes can match the simulated solar light [28–31]. In addition, 4,7-dibromo-2,1,3-benzothiadiazole is very reactive for nucleophilic substitution reactions and coupling reactions [32]. Benzothiadiazole functionalized dyes are readily accessible. The side groups on benzothiadiazole-based molecules affect the HOMO level. Inserting fluorine lowers the HOMO,

but introducing alkoxy raises it [33]. Using long-wavelength benzothiadiazole functionalized molecules to interact with UV photoinitiator are promising for application in sensitization of curing systems upon visible light. Their flexible molecular orbital energy levels have a positive influence on matching with iodonium salt to generate synergistic effect.

In this study, a series of visible-light curing systems based on two benzothiadiazole dyes with different ratios of IOPF were designed. Facile synthesis of the two benzothiadiazole dyes was accomplished in our laboratory. Near-infrared (NIR) and UV–visible spectroscopy technologies were utilized for detecting epoxy conversion of E51 and photolysis of photoinitiator, dye and their mixtures, respectively. In the light curing study, cationic photopolymerization of E51 were investigated under a 470-nm light emitting diode (LED) irradiator in the absence and presence of 510-nm light filter. The influence of dye absorption, the photoelectron transfer reaction between IOPF and dyes and sample thickness on the curing systems of E51 were studied, and discussion for further understanding the structure–property relationship were also involved. There are still few 510-nm photosensitizers for photopolymerization. The two benzothiadiazole dyes have good interact with IOPF under both 470-nm light and 510-nm light, and it is hoped to be a very promising candidate for long-wavelength light curing technology.

Experimental

Materials

The materials and agents used were as follows: diphenyliodonium hexafluorophosphate (IOM, cationic photoinitiator, TCI (Shanghai) Chemical Industry Development Co., Ltd.); benzothiadiazole dyes (**Y-1** and **Y-2**) were prepared in our laboratory; bisphenol-A epoxy resin (E51, photosensitive resin, Jiangsu Sanmu Group Co. Ltd.); epichlorohydrin (C_3H_5ClO, chemical pure, Beijing Chemical Works). The initial material 4,7-dibromo-2,1,3-benzothidiazole is purchased from Energy Chemical (Beijing). Tetrabutylammoniun hexafluorophosphate (n-Bu_4NPF_6) of 0.1 M was added into a dichloromethane solution (DCM) as electrolyte, which was purchased from Tokyo Chemical Industry Co., Ltd. (Tianjin), for cyclic voltammetry (CV) measurements.

Synthesis of benzothiadiazole dyes

The synthetic route of **Y-1** and **Y-2** is shown in Scheme 1. The intermediates 1 and 2 are prepared according to literatures [34–37].

Synthesis of **1** and **Y-1**: 10-mmol p-fluorobromobenzene, 20-mmol KOH and 20-mL DMSO solution were sequentially added into a one-neck round flask of 100 mL to form a mixture, which was stirred 10 min at room temperature. Then, 10 mmol of p-fluoroaniline was added to the system. Their reactions lasted 2 h at room temperature in the dark. Finally, products were obtained by extracting three

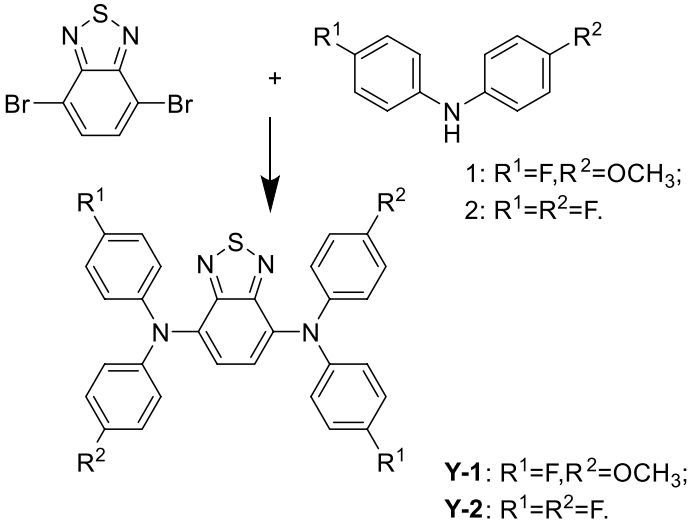

Scheme 1 The synthesis route of **Y-1** and **Y-2**

times with a water/ethyl acetate mixture of 40/20 mL, and the organic solvent was removed without purification. Then, 1.0 mmol 4,7-dibromo-2,1,3-benzothidiazole, 3.0 mmol compound 2, 0.9-g $Pd_2(dba)_3$, 448-mg t-BuOK, 0.14-mL P(t-Bu)$_3$ and 30-mL toluene reacted 12 h in a 100-mL two-neck flask under argon. After the reaction product was extracted with ethyl acetate, the extracts passed through a column (PE: EA = 20:1).

Y-1: This was ^{1}H NMR (400 MHz, DMSO-d_6) δ 7.15–7.10 (m, 10H), 7.03 (m, 8H). ^{13}C NMR (101 MHz, CDCl3) δ 162.09, 159.68, 154.07, 145.92, 145.89, 137.65, 131.82, 127.18, 127.10, 125.88, 118.01, 117.79.

Synthesis of **2** and **Y-2**: The synthetic procedure of **2** and **Y-2** is the same as Synthesis of **1** and **Y-1**, 10-mmol p-methoxybromobenzene was used instead of 10-mmol p-fluorobromobenzene.

Y-2: this was ^{1}H NMR (400 MHz, DMSO-d_6) δδ 7.08–7.03 (m, 10H), 6.91-6.87 (m, 8H), 3.73 (s, 6H).^{13}C NMR (101 MHz, CDCl3) δ 158.21, 154.09, 146.49, 142.89, 137.66, 128.04, 126.03, 125.95, 125.47, 117.74, 117.52, 116.61, 57.43.

UV–Vis absorption, fluorescence emission spectroscopic and CV measurements

IOPF, dyes and E51 were weighed and fully mixed, and samples include IOM/**Y-I**/E51, IOM/**Y-2**/E51, IOM/E51, **Y-1**/E51 and **Y-1**/E51.UV–vis absorption spectra were measured by UV-2600 UV–vis spectrophotometer (Shimadzu, Japan). Absorption changes with irradiation time were measured for dichloromethane solution of IOPF, dyes and IOPF/dye/E51 under a light source (FUV-6BK UV curing machine connecting with light emitting diode (LED) irradiator (470 nm), Guangzhou Banwoo Electronic Technology Co., Ltd.). The fluorescence emission spectra of **Y-1** and

Y-2 are also compared. The fluorescence spectra conducted on a F-4500 fluorescence spectrophotometer (Hitachi, Japan) were used.

The CV tests were performed on a Zennium electrochemical workstation (ZAHNER, Germany) using a three-electrode system. Oxidation and reduction potentials of **Y-1** and **Y-2** were determined by cyclic voltammetry (CV) in acetonitrile solutions containing 0.1 M NBu_4PF_6 as a supporting electrolyte.

NIR spectroscopy measurement

NIR spectroscopy was performed on a 5700 infrared spectrometer (Nicolet, USA) to analyze the curing samples to detect the characteristic absorption peaks changes for the epoxy group of E51 with illumination time. The sample prepared was placed in a plastic round-hole mold with a diameter of 6 mm. An average value was determined from three repeated NIR tests. The light source for cationic light curing was an LED irradiator with a wavelength of 470 nm (110 mW cm^{-2}, A single-channel UV-A illuminometer, Beijing Normal University Optoelectronic Instrument Factory). When a filter was used, it was placed between the LED irradiator and the sample. The epoxy conversions were calculated by detecting the characteristic absorption peak of epoxy groups (at 6071 cm^{-1}) with illumination time [25, 26]. The equation is as below.

$$\text{Epoxy conversion } \% = \left[1 - \left(S_T/R_T\right)/\left(S_0/R_0\right)\right] \times 100\%$$

where S_T is the area of the epoxy C–H characteristic absorbance peak, S_0 is the initial area of the epoxy C–H characteristic absorbance peak, R_T is the area of the reference peak (at 4678 cm^{-1}) and R_0 is the initial area of the reference peak.

Thermal stability test

Thermal stability study for the products of IOPF/**Y-1**/E51 and IOPF/**Y-2**/E51 after cured was investigated by thermogravimetry (TG) analyses. TG curves were performed on TG 209 F3 Tarsus (NETZSCH, Germany) at a heating rate of 10 °C/min under a nitrogen atmosphere.

Results and discussion

Absorption, fluorescence emission spectra and cyclic voltammograms of Y-1 and Y-2

The synthetic **Y-1** and **Y-2** was characterized by ^{1}H NMR and ^{13}C NMR spectra, as shown in Supplementary Materials. As shown in Fig. 1a, b, **Y-1** has a stronger absorption band than **Y-2**, while much weaker fluorescence emission than that of **Y-2** when at the same concentration. UV–vis absorption spectrum of IOPF of 10^{-4} M in dichloromethane is shown in Fig. 1c. The absorption of IOPF is limited at UV region. It is necessary for IOPF to induce visible light curing by incorporating with long-wavelength dyes. In our studied dyes, the –F and $–OCH_3$-terminated

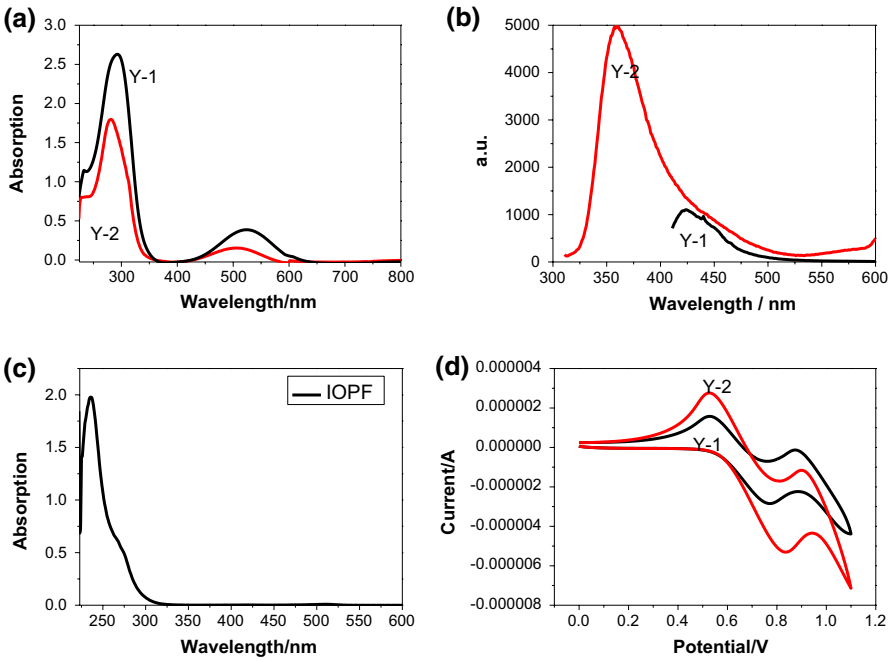

Fig. 1 UV-Vis absorption (**a**) and fluorescence emission spectra (**b**) of **Y-1** and **Y-2** in dichloromethane with concentrations of 10^{-4} M. **c** UV–vis absorption spectra of IOPF of 10^{-4} M in dichloromethane. **d** Cyclic voltammograms of **Y-1** and **Y-2** in dichloromethane

substitutes have an impact on their spectral properties. The visible-light absorption of **Y-1** and **Y-2** is exhibited by the distinct peak at 524 and 506 nm, respectively. The influence of dye structure on their electrochemical behavior was evaluated by

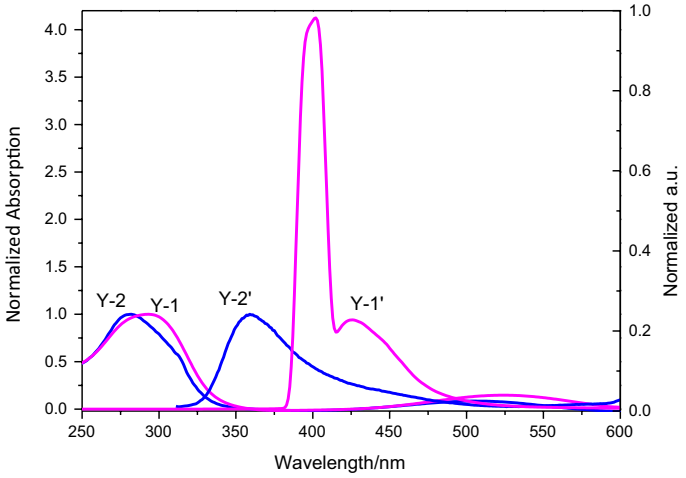

Fig. 2 Normalized absorption, fluorescence emission spectra of **Y-1** and **Y-2** in dichloromethane

CV method, as shown in Fig. 1d. The first oxidation potentials of **Y-1** and **Y-2** are 0.874 V and 0.899 V. Figure 2 displays the normalized absorption and fluorescence emission spectra of **Y-1** and **Y-2** in dichloromethane. The smaller band gap of **Y-1** than **Y-2** suggests that a stronger conjugation was obtained by introducing two methoxy groups. This is consistent with its redshift maximum absorption peak. For their energy levels, the optical band gap (E_g^{opt}) of **Y-1** and **Y-2** are calculated to be 3.45 and 3.76 eV by measuring the intersection wavelength of absorption and fluorescence spectra in Fig. 2 [38]. The above-spectroscopic and electrochemical data of **Y-1** and **Y-2** are listed in Table 1. Based on the Rehm–Weller equation, the free energy changes (ΔG_{el}) for the photoelectron transfer reaction between the excited states of **Y-1**/**Y-2** and IOPF were separately calculated. The reduction potential of IOPF is −0.653 V [39]. The calculated values of ΔG_{el} are negative for IOPF/**Y-1** and IOPF/**Y-2**. Therefore, the photoelectron transfer between IOPF and the studied dyes is thermodynamically allowed.

Theoretical calculations and thermal properties

To gain insight into the electronic properties and geometries of **Y-1** and **Y-2**, quantum chemical calculations based on DFT at the B3LYP/6-31G level were carried out. The optimized geometric structures and frontier orbital of **Y-1** and **Y-2** are shown in Fig. 3. From Fig. 3a, the dihedral angles between the benzothiadiazole core and the diphenylamine of **Y-1** are (C20–C12–N10–C3, 39.609°) and (C35–C14–N11–C6, 42.953°), and those of **Y-2** are (C20–C12–N10–C3, 40.115°) and (C35–C14–N11–C6, 40.115°). The bond lengths between the benzothiadiazole core and the diphenylamine of **Y-1** are (1.414 Å, N10–C3) and (1.415 Å, N11–C6), and those of **Y-2** are (1.416 Å, N10–C3) and (1.416 Å, N11–C6). The result is attributed to **Y-2** incorporating bis(4-fluorophenyl)amine having a very symmetric configuration as compared to **Y-1** with 4-fluoro-*N*-(4-methoxyphenyl)aniline. Both Y-1 and Y-2 have a capability of photoinduced electron transfer by the HOMO–LUMO excitation, according to and frontier orbital results from Fig. 3b. The highest occupied molecular orbital (HOMO) of **Y-1** and **Y-2** almost delocalize over the whole molecule, while the lowest unoccupied molecular orbital (LUMO) is localized at the benzothiadiazole core.

Photopolymerization

NIR technology was utilized to study the variation in epoxy conversion with illumination time for the visible-curing systems: IOPF/**Y-1**/E51 and IOPF/**Y-2**/E51. The

Table 1 Photochemical and electrochemical data of Y-1 and Y-2

Name	λ_{max}^{abs}/nm		λ_{max}^{fl}/nm	E_{ox}/V		E_{red}/V	E_g^{opt}/eV	ΔG_{el}/eV
Y-1	293	525	426	0.874	0.529	0.767	3.45	− 1.93
Y-2	281	506	360	0.899	0.527	0.837	3.76	− 2.21

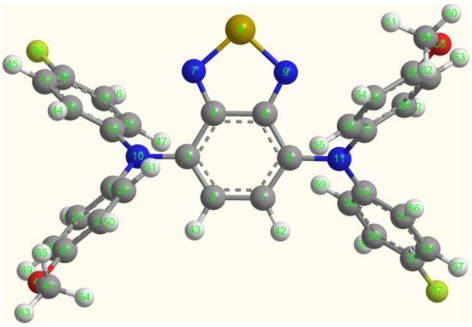

Y-1

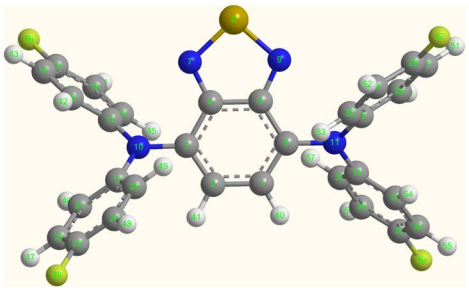

Y-2

(a)

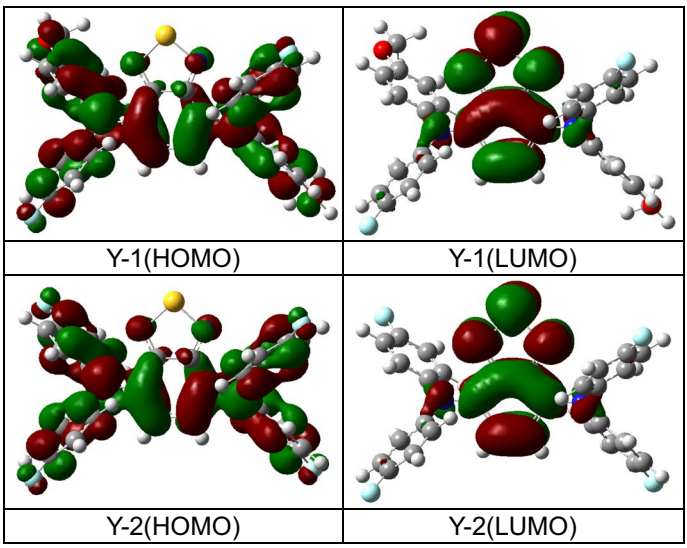

(b)

Fig. 3 Optimized geometric structures (**a**) and frontier orbitals (**b**) of **Y-1** and **Y-2**

effects of IOPF/benzothiadiazole-based organic dyes ratio, sample thickness and different light irradiation on the curing systems of cationic polymerization of E51 were investigated. The curing systems of IOPF/E51, **Y-1**/E51 and **Y-2**/E51 are also analyzed for comparison. A LED light irradiator with the wavelength of 470 nm was applied for our research. A filter of 510 nm with transmittance about 86% were subsequently used, and the measured transmittance value is shown in Supplementary Materials (Fig. S1).

Figure 4a shows the epoxy conversion of E51 as a function of irradiation time under 470-nm LED irradiator. The amount of IOPF and two organic dyes are 2.0 wt.% and 1.0 wt.%, separately. At 470-nm light with intensity of 110 mW cm^{-2} and sample thickness of 120 μm, E51 conversions reach up to 94.3% and 94.9% by IOPF sensitized by **Y-1** and **Y-2**. IOPF/Y-2/E51 exhibits a faster curing rate than IOPF/**Y-1**/E51. This result may be related to the photoelectron transfer between IOPF and the studied dyes. As calculated in section "Absorption, fluorescence emission spectra and cyclic voltammograms of **Y-1** and **Y-2**," the calculated free energy changes (ΔG_{el}) for the photoelectron transfer reaction between the excited states of **Y-2** and IOPF (−2.1 eV) is more negative than that between the excited states of **Y-1** and IOPF (−1.93 eV), suggesting higher reactivity for IOPF and **Y-2** [25]. In addition, the curing results of polymerizations in the IOPF/E51, **Y-1**/E51 and **Y-2**/

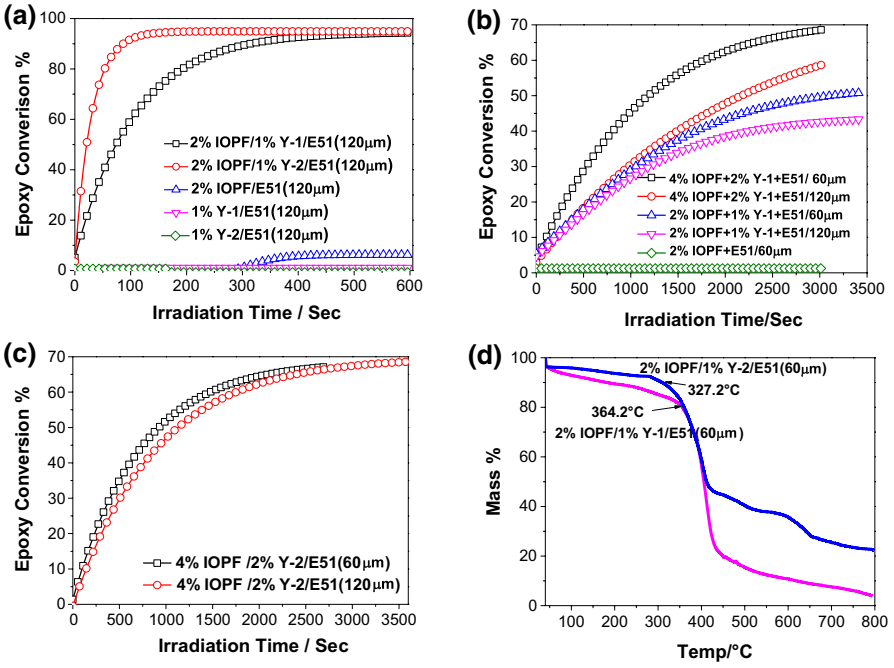

Fig. 4 **a** Epoxy conversions of E51 under 470-nm LED irradiator with increasing irradiation time; **b** Epoxy conversions of E51 initiated by IOPF/Y-1, IOPF **c** IOPF/Y-2 in the presence of 510-nm filter; and **d** TG analyses of IOPF/Y-1/E51 and IOPF/Y-2/E51 in the presence of 510-nm filter. The percentages of IOPF, Y-1 and Y-2 are mass fraction

E51 system show that IOPF initiated E51 alone achieves conversion about 6.2%, and also the **Y-1**/E51 and **Y-2**/E51 systems cannot induce E51 alone under LED light.

In order to further understand the structure–conversion relationship of the studied curing systems, a 510-nm filter was put between the LED irradiator and the sample. Different ratios of IOPF/benzothiadiazole dyes and sample thickness were investigated for the curing systems. The curing results of IOPF/**Y-1**/E51 and IOPF/**Y-2**/E51 systems are shown in Fig. 4b, c. In the presence of 510-nm filter, both the IOPF/**Y-1**/E51 and IOPF/**Y-2**/E51 system approach epoxy conversions close to 70%. In Fig. 4b, the concentration of IOPF and **Y-1** has greatly influenced the epoxy conversion in IOPF/**Y-1**/E51 systems. Although the concentration ratio of IOPF/**Y-1** are the same as 2:1, the IOPF of 4 wt.% with sensitization by **Y-1** of 2 wt.% exhibits much faster initiation performance than IOPF of 2 wt.% with **Y-1** of 1 wt.%. The increase in concentrations of photoinitiator and photosensitizer greatly enhanced the curing performance of E51 under filter. Meanwhile, IOPF/**Y-1** initiated E51 more efficiently at 60-μm sample thickness than that at 120-μm sample thickness. The photoinitiation rate of IOPF/**Y-1** is apparently influenced by changing sample thickness. In contrast, the IOPF of 4 wt.% with sensation by **Y-2** of 2 wt.% exhibits good initiation performances at both 60-μm and 120-μm sample thicknesses, as shown in Fig. 4c. The photoinitiation rate of IOPF with **Y-2** at 60-μm sample thickness is only a little faster than at 120-μm simple thickness. On the whole, curing systems based on **Y-2** have better activity than those based on **Y-1** under the long-wavelength light of 470 nm and 510 nm. As known, IOPF have no absorption at 470 nm and 510 nm. **Y-1** has wider absorption band range, but maybe a stronger synergistic interaction occurs between IOPF and **Y-2** than that between IOPF and **Y-1**.

Besides, the products after cured under 510-nm filter of IOPF/**Y-1**/E51 and IOPF/**Y-2**/E51 show good properties on thermal stability. Based on TG analyses in Fig. 4d, IOPF/Y-1/E51 and IOPF/Y-2/E51 display a thermal decomposition temperature (T_d) of 364.2 °C and 327.2 °C, and the weight losses during TG are 15% and 4% upon heating up to 300 °C, respectively. Y-1 and y-2 sensitized IOPF not only accelerated the curing of E51, but also obtained the curing polymer with high thermal stability [25]. IOPF/benzothiadiazole dyes are very promising candidate photoinitiation system for visible light curing beyond 500 nm. This work is hoped to provide experimental basis for such long-wavelength irradiated curing applications.

Synergistic effect of IOPF and benzothiadiazole dyes

UV–vis absorption spectra were employed to compare the absorption peak changes of IOPF/benzothiadiazole dyes mixtures and benzothiadiazole dyes alone before and after illumination. The interaction between IOPF and benzothiadiazole dyes was further studied. Figure 5 presents normalized absorption changes with illumination time of IOPF/**Y-1**, IOPF/**Y-2**, **Y-1** and **Y-2** in solution, respectively. The absorbance was measured at a certain interval.

Figure 5a shows a new absorption at 600–800 nm increases at first and then gradually decreases for IOPF/**Y-1**, so as that shown in Fig. 5b for IOPF/**Y-2**. The decreasing change of absorption at around 510 nm favors the synergistic effect of

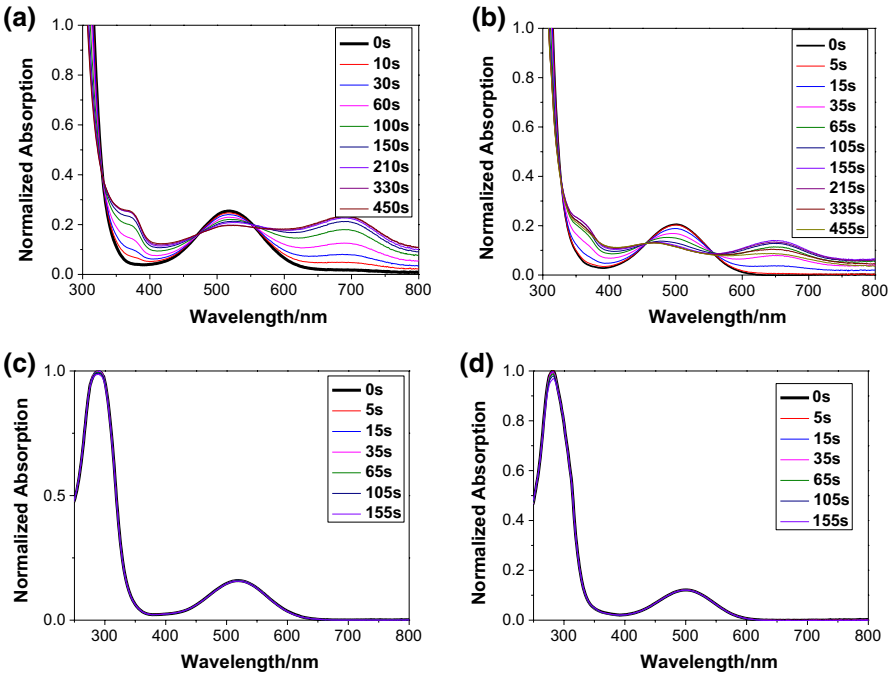

Fig. 5 Photolysis of **a** IOPF/**Y-1**, **b** IOPF/**Y-2**, **c** **Y-1** and **d** **Y-2** in epichlorohydrin

Y-1 and **Y-2** on sensitizing IOPF even in the presence of the filter. The results indicate consumption of dyes occurs under interactions with IOPF. As a comparison, Fig. 5c, d displays the main absorption of Y-1 and Y-2 does not change with prolonged illumination, and there is almost no photolysis in the solution of benzothiadiazole dyes alone. Thus, the synergistic effect of benzothiadiazole dyes with IOPF can be inferred from the phenomena, and it enhances the efficient initiation of E51 to be fast cured under visible light [40].

Conclusions

The synthesized benzothiadiazole dyes (**Y-1** and **Y-2**) assist the UV photoinitiator IOPF in the absorption of visible light, and they can effectively initiate the curing of bisphenol-A epoxy resin (E51) under 470-nm LED irradiator in the absence and presence of 510-nm filter. The parameters of IOPF/**Y-1**/E51 and IOPF/**Y-2**/E51 curing are investigated using NIR spectroscopy and photolysis. **Y-1** has superiority of longer maximum absorption wavelength at 525 nm than that of **Y-2** at 506 nm. However, IOPF/**Y-2** initiated E51 much faster than IOPF/**Y-1**, which is possibly due to easier synergistic effect between IOPF and **Y-2**. The final epoxy conversions of IOM/**Y-1**/E51 and IOM/**Y-2**/E51 curing systems are close to 95% under the 470-nm LED irradiator and even reach 70% in the presence of 510-nm filter. The photolysis

of IOPF and benzothiadiazole dyes has good activity after mixing, from which a synergistic effect between the two is inferred.

Acknowledgements The authors wish to thank Tianjin University of Technology Municipal College Students Innovation and Entrepreneurship Training Program Subsidy Project (201810060068) and the National Natural Science Foundation of China (21506164).

References

1. Pintossi D, Iannaccone G, Colombo A, Bella F, Välimäki M, Väisänen KL, Hast J, Levi M, Gerbaldi C, Dragonetti C, Turri S, Griffini G (2016) Luminescent downshifting by photo-induced sol-gel hybrid coatings: accessing multifunctionality on flexible organic photovoltaics via ambient temperature material processing. Adv Electron Mater 2:1600288
2. Kuang X, Zhao Z, Chen K, Fang D, Kang G, Qi HJ (2018) High-speed 3D printing of high-performance thermosetting polymers via two-stage curing. Macromole Rapid Commun 39:1700809
3. Ravi P, Wright J, Shiakolas PS, Welch TR (2019) Three-dimensional printing of poly(glycerol sebacate fumarate) gadodiamide-poly(ethylene glycol) diacrylate structures and characterization of mechanical properties for soft tissue applications. J Bio Mater Res B 107:664–671
4. Li Z, Wang C, Qiu W, Liu R (2019) Antimicrobial thiol-ene-acrylate photosensitive resins for DLP 3D printing. Photochem Photobiol 95:1219–1229
5. Cheng Q, Zheng Y, Wang T, Sun D, Lin R (2020) Yellow resistant photosensitive resin for digital light processing 3D printing. J Appl Polym Sci 137:48369
6. Chen Z, Wang X, Li S, Liu S, Miao H, Wu S (2019) Near-infrared light driven photopolymerization based on photon upconversion. ChemPhotoChem 3:1077–1083
7. Kitano H, Ramachandran K, Bowden NB, Scranton AB (2013) Unexpected visible-light-induced free radical photopolymerization at low light intensity and high viscosity using a titanocene photoinitiator. J Appl Polym Sci 128:611–618
8. Ge X, Ye Q, Song L, Misra A, Spencer P (2015) Visible-light initiated free-radical/cationic ring-opening hybrid photopolymerization of methacrylate/epoxy: polymerization kinetics, crosslinking structure, and dynamic mechanical properties. Macromol Chem Phys 216:856–872
9. Corrigan N, Yeow J, Judzewitsch P, Xu J, Boyer C (2019) Seeing the light: advancing materials chemistry through photopolymerization. Angew Chem Int Ed 58:5170–5189
10. Dressano D, Palialol AR, Xavier TA, Braga RR, Oxman JD, Watts DC, Marchi GM, Lima AF (2016) Effect of diphenyliodonium hexafluorophosphate on the physical and chemical properties of ethanolic solvated resins containing camphorquinone and 1-phenyl-1,2-propanedione sensitizers as initiators. Dent Mater 32:756–764
11. Sari E, Mitterbauer M, Liska R, Yagci Y (2019) Visible light induced free radical promoted cationic polymerization using acylsilanes. Prog Org Coat 132:139–143
12. Corakci B, Hacioglu SO, Toppare L, Bulut U (2013) Long wavelength photosensitizers in photoinitiated cationic polymerization: the effect of quinoxaline derivatives on photopolymerization. Polymer 54:3182–3187
13. Fang B, Jin M, Wu X, Zhang Y, Wan D (2016) Near UV–vis LED-excitable two-branched sensitizers for cationic, radical, and thiol-ene photopolymerizations. Dyes Pigments 126:54–61
14. Mokbel H, Dumur F, Raveau B, Morlet-Savary F, Simonnet-Jégat C, Gigmes D, Toufaily J, Hamieh T, Fouassier JP, Lalevée J (2016) Perovskites as new radical photoinitiators for radical and cationic polymerizations. Tetrahedron 72:7686–7690
15. Shen W, Wang L, Cao Y, Zhang L, Yang Z, Yuan X, Yang H, Jiang T, Chen H (2019) Cationic photopolymerization of liquid crystalline epoxide in mesogenic solvents and its application in polymer-stabilized liquid crystals. Polymer 172:231–238
16. Golaz B, Michaud V, Leterrier Y, Månson JAE (2012) UV intensity, temperature and dark-curing effects in cationic photo-polymerization of a cycloaliphatic epoxy resin. Polymer 53:2038–2048
17. Liu X, Guo J, Sun J, Gu X, Feng W, Liu W, Li H, Zhang S (2019) The preparation of a bisphenol A epoxy resin based ammonium polyphosphate ester and its effect on the char formation of fire resistant transparent coating. Prog Org Coat 129:349–356

18. Musa A, Alamry KA, Hussein MA (2019) The effect of curing temperatures on the thermal behaviour of new polybenzoxazine-modified epoxy resin. Polym Bull. https://doi.org/10.1007/s00289-019-03026-0
19. Selvi M, Devaraju S, Alagar M (2019) Cyclotriphosphazene nanofiber-reinforced polybenzoxazine/epoxy nanocomposites for low dielectric and flame-retardant applications. Polym Bull 76:3785–3801
20. Liu G, Zhu X, Xu B, Qian X, Song G, Nie J (2013) Cationic photopolymerization of bisphenol A diglycidyl ether epoxy under 385 nm. J Appl Polym Sci 130:3698–3703
21. Morita Y (2005) Cationic polymerization of hydrogenated bisphenol-A glycidyl ether with cycloaliphatic epoxy resin and its thermal discoloration. J Appl Polym Sci 97:1395–1400
22. Wang T, Wang ZH (2005) Cationic photopolymerization of epoxy systems initiated by cyclopentadien-iron-biphenyl hexafluorophosphate ([Cp-Fe-biphenyl]$^{+}PF_6^{-}$). Polym Bull 53:323–331
23. Abadie MJM, Chia NK, Boey F (2002) Cure kinetics for the ultraviolet cationic polymerization of cycloliphatic and diglycidyl ether of bisphenol-A(DGEBA) epoxy systems with sulfonium salt using an auto catalytic model. J Appl Polym Sci 86:1587–1591
24. Vabrik R, Czajlik I, Túry G, Rusznák I, Ille A, Víg A (1998) A study of epoxy resin–acrylated polyurethane semi-interpenetrating polymer networks. J Appl Polym Sci 68:111–119
25. Chen Y, Jia X, Wang M, Wang T (2015) A synergistic effect of a ferrocenium salt on the diaryliodonium salt-induced visible-light curing of bisphenol-A epoxy resin. RSC Adv 5:33171–33176
26. Wang M, Ma X, Yu J, Jia X, Han D, Zhou T, Yang J, Nie J, Wang T (2015) Aromatic amine-sulfone/sulfoxide conjugated D–π–A–π-D-type dyes in photopolymerization under 405 nm and 455 nm laser beams. Polym Chem 24:4424–4435
27. Schmitz C, Halbhuber A, Keil D, Strehmel B (2016) NIR-sensitized photoinitiated radical polymerization and proton generation with cyanines and LED arrays. Prog Org Coat 100:32–46
28. Huang H, Chen H, Long J, Wang G, Tan S (2016) Novel D–A–π–A organic dyes based on 3-dimensional triarylamine and benzothiadiazole derivatives for high-performance dye-sensitized solar cells. J Power Sources 326:438–446
29. Li F, Chen Y, Zong X, Qiao W, Fan H, Liang M, Xue S (2016) New benzothiadiazole-based dyes incorporating dithieno[3,2-b:2′,3′-d]pyrrole (DTP) π-linker for dye-sensitized solar cells with different electrolytes. J Power Sources 332:345–354
30. Pathaka A, Tomera T, Thomas KRJ, Fan MS, Ho KC (2019) Fine tuning the absorption and photovoltaic properties of benzothiadiazole dyes by donor-acceptor interaction alternation via methyl position. Electrochim Acta 304:1–10
31. Fernandes SSM, Pereira A, Ivanou D, Mendes A, Raposo MMM (2018) Benzothiadiazole derivatives functionalized with two different (hetero)aromatic donor groups: synthesis and evaluation as TiO_2 sensitizers for DSSCs. Dyes Pigments 151:89–94
32. Li M, An C, Pisula W, Müllen K (2018) Cyclopentadithiophene-benzothiadiazole donor – acceptor polymers as prototypical semiconductors for high-performance field-effect transistors. Acc Chem Res 51:1196–1205
33. Wang N, Chen Z, Wei W, Jiang Z (2013) Performance polymer solar cells without any processing additives or post-treatments. J Am Chem Soc 135:17060–17068
34. Wang J, Chen Y, Li F, Zong X, Guo J, Sun Z, Xue S (2016) A new carbazole-based hole-transporting material with low dopant content for perovskite solar cells. Electrochim Acta 210:673–680
35. Ahn M, Kim MJ, Wee KR (2019) Electron push–pull effects in 3,9-bis(p-(R)-diphenylamino) perylene and constraint on emission color tuning. J Org Chem 84:12050–12057
36. Woon KL, Nadiah ZN, Hasan ZA, Ariffin A, Chenc SA (2016) Tuning the singlet-triplet energy splitting by fluorination at 3,6 positions of the 1,4-biscarbazoylbenzene. Dyes Pigments 132:1–6
37. Chen W, Zhang S, Dai G, Chen Y, Li M, Zhao X, Chen Y, Chen L (2019) Tuning the photophysical properties of symmetric squarylium dyes: investigation on the halogen modulation effects. Chem Eur J 25:469–473
38. Tan YL, Liang M, Lu ZY, Zheng YQ, Tong XL, Sun Z et al (2014) Novel triphenylamine donors with carbazole moieties for organic sensitizers toward cobalt(II/III) redox mediators. Org Lett 16:3978–3981
39. Ignatenko VY, Ilyin SO, Kostyuk AV, Bondarenko GN, Antonov SV (2019) Acceleration of epoxy resin curing by using a combination of aliphatic and aromatic amines. Polym Bull. https://doi.org/10.1007/s00289-019-02815-x

40. Liu R, Xu Y, Jia J, Chen P, Zhang F, Zhang L, Chen Y (2020) Improvement on curing performance and morphology of E5I/TPGDA mixture in a free radical-cationic hybrid photopolymerization system. J Polym Res 27:166